

Non-Enhanced MR Angiography of the Lower Extremity Arteries at 7T: Correction of Saturation Pulse Artifacts

Sören Johst^{1,2}, Stephan Orzada^{1,2}, Mark E. Ladd^{1,3}, and Stefan Maderwald¹

¹Erwin L. Hahn Institute for MRI, University Duisburg-Essen, Essen, Germany, ²Diagnostic and Interventional Radiology and Neuroradiology, University Hospital Essen, University Duisburg-Essen, Essen, Germany, ³Medical Physics in Radiology, German Cancer Research Center (dkfz), Heidelberg, Germany

Target Audience:

Researchers working on non-enhanced MR angiography methods / ultra-high field MRI.

Introduction:

The visibility of the vasculature in time-of-flight (TOF) MR angiography (MRA) highly profits from increased field strengths¹. In recently published work, a turbo-FLASH (TFL) sequence was modified for non-contrast-enhanced imaging of the lower extremity vessels² (Fig. 1). To reduce total acquisition time, saturation RF pulses for the suppression of venous signals were applied only every second TR (Fig. 2). This leads to an artifact in axial slices which appears similar to aliasing (Fig. 1). The artifact is caused by periodic signal variation due to alternating TR length.

Material and Methods:

All measurements were performed on a 7T whole-body system (Magnetom 7T, Siemens, Erlangen, Germany) equipped with a custom-built 8-channel Tx/Rx head coil³ using a spherical oil phantom (polydimethylsiloxan) with a T_1 of approximately 1420 ms. The TFL based sequence that was used for in-vivo imaging (Fig. 1) was modified to be able to change the excitation flip angle θ_2 independently (Fig. 2).

Imaging parameters: single slice with 2 mm thickness, nominal flip angle 70° , TE = 3.45 ms, TR = 2020 ms (complete slice), FOV 300 mm x 225 mm, matrix 192 x 144, no parallel image acceleration, bandwidth 930 Hz/px, saturation pulse block placed below imaging slice (gap 20 mm, thickness 80 mm), TR₁ = 7.01 ms and TR₂ = 4.2 ms.

Theory: Steady-state magnetization for TR₁ / TR₂ can be calculated as:

$$M_{ZE,1} = M_0 \cdot \frac{1 + e^{-\frac{TR_1}{T_1}} \left(\left(1 - e^{-\frac{TR_2}{T_1}} \right) \cos \theta_1 - 1 \right)}{1 - \cos \theta_1 \cos \theta_2 e^{-\frac{TR_1 + TR_2}{T_1}}} \quad M_{ZE,2} = M_0 \cdot \frac{1 + e^{-\frac{TR_2}{T_1}} \left(\left(1 - e^{-\frac{TR_1}{T_1}} \right) \cos \theta_2 - 1 \right)}{1 - \cos \theta_1 \cos \theta_2 e^{-\frac{TR_1 + TR_2}{T_1}}}$$

To ensure correct image acquisition, the signal from both excitations with different TR has to be the same. Since the tissue is the same in both cases, the flip angles have to satisfy: $M_{ZE,1} \cdot \sin \theta_2 = M_{ZE,2} \cdot \sin \theta_1$. Thereby, an optimal θ_2 dependent on θ_1 , T_1 and TR₁ / TR₂ can be calculated defined by the minimum of the absolute signal difference $D = |M_{ZE,1} \cdot \sin \theta_2 - M_{ZE,2} \cdot \sin \theta_1|$ (Fig. 3). For the given T_1 (>> TR₁, TR₂), D is mainly determined by the ratio TR₁/TR₂.

Results:

B₁ mapping showed that the actual flip angles ranged from 60° to 90° . Imaging with 75% reduction in θ_2 relative to θ_1 showed qualitatively the lowest overall artifact signal level (Fig. 4). Figure 5 shows normalized measured artifact signal originating from a position inside the phantom with the nominal flip angle θ_1 of 70° for all 17 measurements. These data are compared to the calculated normalized absolute signal difference D . In contrast to the calculated minimum for θ_2 at 85% of θ_1 , the measured artifact signal suggests the minimum to be between 75% and 80% of θ_1 . This agrees with the qualitative comparison of the images, where a 75% reduction of θ_2 also showed the lowest artifact signal of all measurements.

Discussion and Conclusion:

Although the optimal flip angle θ_2 with the lowest artifact level cannot be determined exactly from the measured data because of the noise level in the images, there seems to be a shift towards lower values compared to the theoretical expectation. This needs further investigation e.g. with averaged measurements. On the other hand, the inhomogeneous flip angle distribution at 7T makes it difficult to completely correct this artifact, as every flip angle has its own theoretical reduction factor (Fig. 3). However, the artifact level can be reduced considerably even if the exact reduction is not met (cf. Fig. 5, blue line). Another possibility to further reinforce the artifact reduction/correction would be a special ordering of the k-space data during acquisition or correction factors within the raw data before image reconstruction.

References: 1. Maderwald et al. MAGMA 21:159-167 (2008); 2. Fischer et al. Invest Radiol 48:525-34 (2013); 3. Orzada et al. ISMRM 2009, abstract 3010.

The research leading to these results has received funding from the European Research Council under the European Union's Seventh Framework Programme (FP/2007-2013) / ERC Grant Agreement n. 291903 MRexcite.

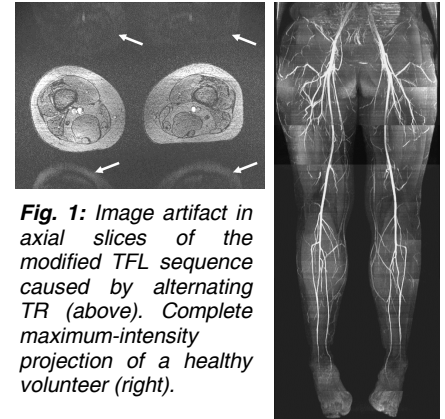


Fig. 1: Image artifact in axial slices of the modified TFL sequence caused by alternating TR (above). Complete maximum-intensity projection of a healthy volunteer (right).

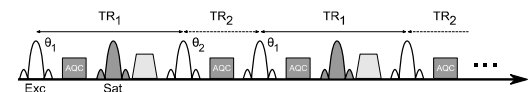


Fig. 2: Diagram of TFL sequence showing variation in effective TR because of the saturation pulse block preceding every second excitation.

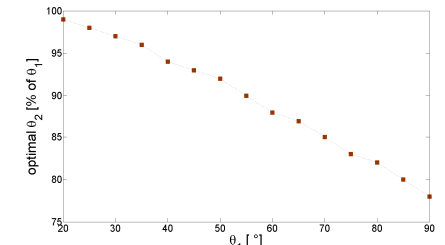


Fig. 3: Calculated optimal flip angle θ_2 for artifact correction defined by the minimum of the absolute signal difference D for TR₁ = 7.01 ms and TR₂ = 4.2 ms.

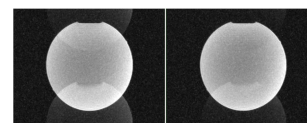


Fig. 4: Artifact in phantom measurements for $\theta_2 = \theta_1$ (left) and $\theta_2 = 75\%$ of θ_1 (right), which showed the lowest overall artifact signal. Both images are windowed identically.

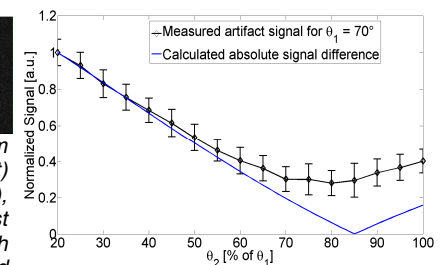


Fig. 5: Measured data for ROI corresponding to θ_1 of approximately 70° (black line) compared to calculated absolute signal difference D between both excitations with θ_1 / θ_2 (blue line). Error bars represent standard deviation within ROI. Both measured and calculated data were normalized to 1.